

IMPORTANCE OF CORRECTION FACTOR ASSOCIATED WITH SEDIMENT CONCENTRATION AND VELOCITY DISTRIBUTION IN DEBRIS FLOW SIMULATIONS

By

Takahiro Itoh and Shinji Egashira

Department of Civil and Environmental Systems Engineering, Ritsumeikan University,
1-1-1 Noji-Higashi, Kusatsu, Shiga 525-8577, Japan

SYNOPSIS

Debris flow characteristics such as flow discharge, mean flow velocity, mean sediment concentration and sediment runoff volume are usually predicted by numerical simulations with the governing equations. Formulas for erosion/deposition rate and flow resistance play important roles in mass and momentum equations. In addition, potential erosion depth and sediment correction factors also affect significantly the debris flow characteristics.

The present study emphasizes the importance of the correction factor associated with sediment concentration and velocity profiles in predicting sediment transport rate and sediment runoff volume. According to Egashira et al.'s constitutive relationship, sediment is concentrated near the bed, and this non-homogeneous increases with decreasing bed slope. This means the flux sediment concentration of a debris flow differs from the volumetric cross-sectional mean concentration. Correspondingly, sediment runoff volume simulated without correction factors is very different from actual runoff volume. In this paper, a method of predicting the correction factor for sediment discharge is presented and simulated results of the runoff process of debris flow in a flume are discussed.

INTRODUCTION

It is very difficult to rationally develop constitutive equations for debris flows and mud flows, because shear stress structures are quite different from shear stress structures of Newtonian fluids. Many constitutive equations, therefore, have been presented. Defining debris flows as mixture flows of water and coarse sediment particles, Itoh et al. (1) compared several constitutive equations from a common viewpoint. They emphasize that Egashira, Miyamoto and Itoh's formulas (2, 3) are the most suitable to be extended to other regimes of sediment-laden flows under a steady and uniform flow condition. For instance, their predicted results for flux sediment concentration changes monotonically in a wide region from debris flow to the bed-load regime in agreement with flume data. The shapes of velocity and sediment concentration distributions affect the flow characteristics.

In order to understand debris flow characteristics such as flow discharge, flow velocity, sediment concentration and sediment runoff volume, a numerical simulation is usually required. Much useful knowledge was obtained using the results of numerical simulation; e.g., Honda et al. (4, 5), Hashimoto et al (6), Nakagawa et al (7) and Takahama et al. (8) in Japan. However, it seems that the importance of the correction factor caused by sediment concentration and velocity profiles has not yet been fully recognized (9). According to our previous study, potential erosion depth and correction factor greatly affect debris flow characteristics. Therefore, sediment runoff volume simulated without a correction factor is very different from actual runoff volume. In the present study, the correction factor is obtained from velocity and sediment concentration profiles, which are calculated by substituting our constitutive equations into the momentum conservation equation in a steady and longitudinally uniform flow. A numerical simulation is conducted employing the correction factor in the continuity equation for sediment volume. The calculated results are compared with flume data in order to examine the validity of our recommended correction factors.

CONSTITUTIVE RELATIONSHIPS AND FLOW NATURE

Constitutive Equations

A steady, longitudinally uniform, uni-directional flow of a sediment-water mixture is illustrated in Fig. 1. The momentum conservation equations for such a simple flow reduce to the following equations. Herein, in Fig. 1, c_s is the volumetric sediment concentration in stationary layer, u = velocity in a flow direction, x is the flow direction and z_b is the bed elevation from horizontal.

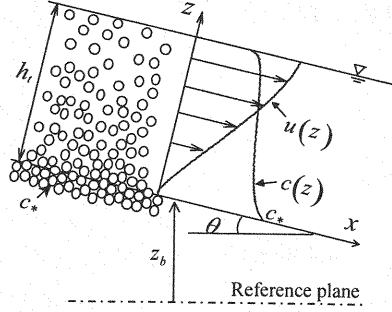


Fig. 1 Schematics of profiles for velocity and sediment concentration in a steady and uniform debris flow over an erodible bed

$$\tau(z) = \int_z^{h_t} \rho_m g \sin \theta dz \quad (1)$$

$$p(z) = \int_z^{h_t} \rho_m g \cos \theta dz \quad (2)$$

in which h_t = flow depth; g = acceleration due to gravity; p = isotropic component of normal stress; z = bed-normal coordinate; θ = inclination from horizontal; and τ = shear stress in planes parallel to the bed. ρ_m = mass density of the sediment and water mixture; $\rho_m = (\sigma - \rho)c + \rho$, in which, σ = mass density of sediment; ρ = mass density of water; and c = sediment concentration by volume.

Egashira et al. (2, 3) and Miyamoto (10) suggest that energy dissipation in debris flows is mainly dominated by static interparticle contacts, inelastic particle collisions and turbulence of interstitial water, which leads to

$$\tau(z) = \tau_y(z) + \tau_d(z) + \tau_f(z) \quad (3)$$

$$p(z) = p_s(z) + p_d(z) + p_w(z) \quad (4)$$

in which τ_y = yield stress; τ_d = shear stress due to inelastic particle-particle collisions; τ_f = shear stress supported by interstitial water; p_s = pressure of static interparticle contacts; p_d = dynamic pressure due to inelastic particle collisions; and p_w = pressure of water. If the turbulent suspension of particles is negligibly small, and thus the particle motion is laminar, the pore water pressure, p_w , is approximately hydrostatic. These stresses are described as follows:

$$\tau_y = p_s \tan \phi_s \quad (5)$$

$$\tau_d = \sigma k_d (1 - e^2) c^{1/3} d^2 \left| \frac{\partial u}{\partial z} \right| \frac{\partial u}{\partial z} \quad (6)$$

$$\tau_f = \rho k_f \frac{(1-c)^{5/3}}{c^{2/3}} d^2 \left| \frac{\partial u}{\partial z} \right| \frac{\partial u}{\partial z} \quad (7)$$

$$p_d = \sigma k_d e^2 c^{1/3} d^2 \left(\frac{\partial u}{\partial z} \right)^2 \quad (8)$$

$$p_w(z) = \rho g (h_t - z) \cos \theta \quad (9)$$

$$p_s / (p_d + p_s) = (c/c_*)^{1/5} \quad (10)$$

in which ϕ_s = interparticle friction angle; e = coefficient of interparticle restitution; d = sediment particle size; u = velocity in a flow direction; c = sediment concentration by volume; k_d = constant ($k_d = 0.0828$) (10); k_f = an

empirical constant ($k_f=0.16$); and c_* = volumetric sediment concentration in the stationary layer as shown in Fig. 1.

Profiles of Velocity, Sediment Concentration and Shear Stress

Substituting Eqs. (5) to (9) into Eqs. (1) and (2) yields

$$p_s \tan \phi_s + \rho(f_d + f_f)d^2 \left| \frac{\partial u}{\partial z} \right| \frac{\partial u}{\partial z} = \int_z^{h_t} \rho \{ (\sigma/\rho - 1)c + 1 \} g \sin \theta dz \quad (11)$$

$$p_s + \rho f_{pd} d^2 \left(\frac{\partial u}{\partial z} \right)^2 = \int_z^{h_t} \rho (\sigma/\rho - 1) c g \sin \theta dz \quad (12)$$

in which $f_d = k_d(1 - e^2)(\sigma/\rho)c^{1/3}$; $f_f = k_f(1 - c)^{5/3}c^{-2/3}$; and $f_{pd} = k_d e^2(\sigma/\rho)c^{1/3}$.

The equations for velocity and sediment concentration distributions are obtained with Eqs. (10), (11) and (12) as follows:

$$\frac{\partial u'}{\partial z'} = \frac{h_t}{d} \left[\frac{G - Y}{f_d + f_f} \right]^{1/2} \quad (13)$$

$$(1 - z') \frac{\partial F}{\partial c} \frac{\partial c}{\partial z'} = F - c \quad (14)$$

in which $z' = z/h_t$; $u' = u/\sqrt{gh_t}$; $G = \sin \theta \int_{z'}^1 \{ (\sigma/\rho - 1)c + 1 \} dz'$;

$Y = (c/c_*)^{1/5} \cos \theta \tan \phi_s \int_{z'}^1 (\sigma/\rho - 1) c dz'$; $F = f_{pd} \tan \theta / [(\sigma/\rho - 1)(F_1 - F_2)]$;

$F_1 = f_f + f_d - f_{pd} \tan \theta$; and $F_2 = (c/c_*)^{1/5} (f_f + f_d - f_{pd} \tan \theta)$.

The velocity and sediment concentration profiles in debris flows over rigid and erodible beds are derived by solving Eqs. (13) and (14) using suitable bottom boundary conditions such as $u = 0$ and $c = c_*$ in erodible cases and $u = 0$ in rigid bed cases (3).

In Fig 2, suitably normalized profiles of velocity, sediment concentration and shear stress are shown for flow over an erodible bed. In the figure, u_s is the velocity at the free surface and τ_b is the bed shear stress. The parameters of the computation are specified as $\theta = 15.0$ deg., $h_t/d = 10$, $c_* = 0.524$, $e = 0.85$. Figure 3 shows the computed results for relationships between the flux sediment concentration, c_f , and bed slope, θ , with same parameters used in the computation of Fig. 2 except bed slope. The flux sediment concentration is defined as $c_f \equiv q_s/q_m = \int_0^{h_t} c u dz / \int_0^{h_t} u dz$ (q_s = sediment discharge rate, q_m = flow rate) (2, 3), and depends on the bed slope in the flow over an erodible bed. The value is numerically obtained by substituting the calculated results in

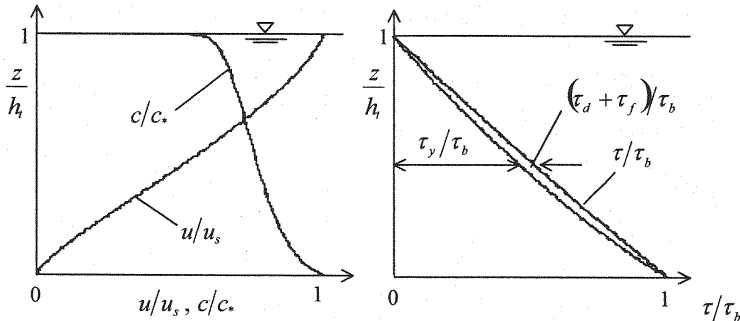


Fig. 2 Profiles of velocity, sediment concentration and shear stress in the debris flow over an erodible bed (Exact solutions)

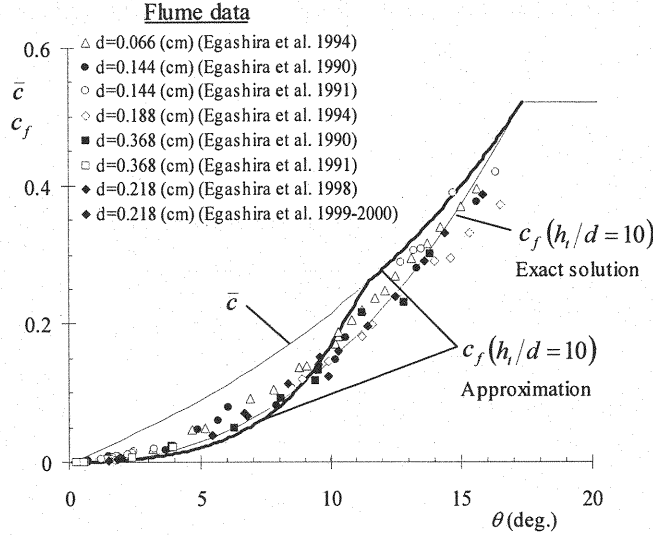


Fig. 3 Calculated curve for relation between mean sediment concentration and sediment flux concentration and equilibrium bed slope

terms of Eqs. (13) and (14) into this equation. This solution is called the “Exact solution”. In comparison to c_f , the cross sectional averaged sediment concentration, \bar{c} , defined as the following equation (2, 3) is shown in the figure, and it is defined as follows:

$$\bar{c} = \frac{\tan \theta}{(\sigma/\rho - 1)(\tan \phi_s - \tan \theta)} \quad (15)$$

As can be seen from Fig. 2, the effect of the shapes of velocity and sediment concentration distributions on the sediment flux is dominant near the bed and the free surface because these characteristics depend on the distribution of shear stress, especially that of yield stress. These features cause the difference between \bar{c} and c_f in Fig. 3. Moreover, the curves not only of the exact solution but also of the approximation agree very well with flume data obtained by the authors. Herein, the solutions solved under the condition that the sediment concentration is vertically uniform are called “Approximation”. The approximated solutions are discussed in the next paragraph.

Figure 4 shows comparison of velocity, sediment concentration and shear stress distributions in wide flow regime from debris flow to flow with bed loads on the erodible bed under the several kinds of bed slope: $\theta = 15, 11, 9.9$ and 3 degrees. Those profiles are calculated with same parameters used in the computation of Fig. 2 except bed slope. In the flow regime with a bed slope less than 12 to 14 degrees, the clear water layer forms near the free surface and the hyper-concentrated sediment-water mixture layer forms near the bed surface, though sediment particles disperse from the bed to the free surface in the debris flow with more than 12 to 14 degree's bed slope. Assuming that the sediment concentration profile in the hyper-concentrated layer is linear distribution in the sediment flow with hyper-concentrated layer and clear water layer, the mean value of sediment concentration in the hyper-concentrated layer is approximately treated as $c_*/2$ (2, 3), and it is possible that the profile of sediment concentration in sediment-water mixture layer is assumed to be a vertically uniform distribution in the debris flow and the sediment flow. In the approximated solution, it is easy to obtain the velocity distribution and the equation of flow resistance and to evaluate the flow characteristic of debris flow, though there are some differences caused by the yield stress distribution near the bed surface as shown in Fig. 4. Ultimately, the “Approximation” is calculated under the following conditions for the mean value of sediment concentration in the hyper-concentrated layer with sediment and water mixture: \bar{c} in case of $\bar{c} > c_*/2$ and $c_*/2$ in case of $\bar{c} \leq c_*/2$.

In case of debris flow, the mean value of sediment concentration is approximately treated as \bar{c} shown in Eq. (15). The mean velocity is analytically obtained by solving Eq. (13).

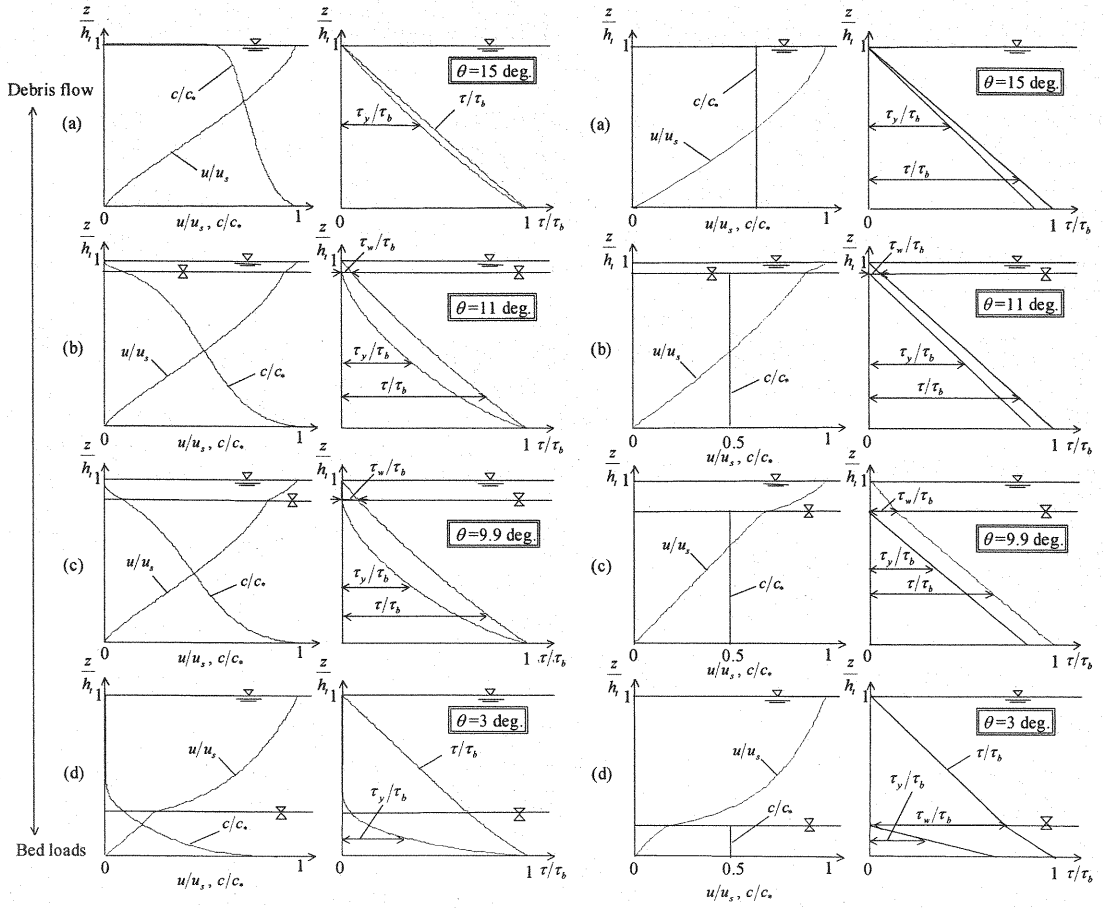


Fig. 4 Comparison of exact solutions and approximations for velocity, sediment concentration and shear stress distributions in the debris flow over an erodible bed

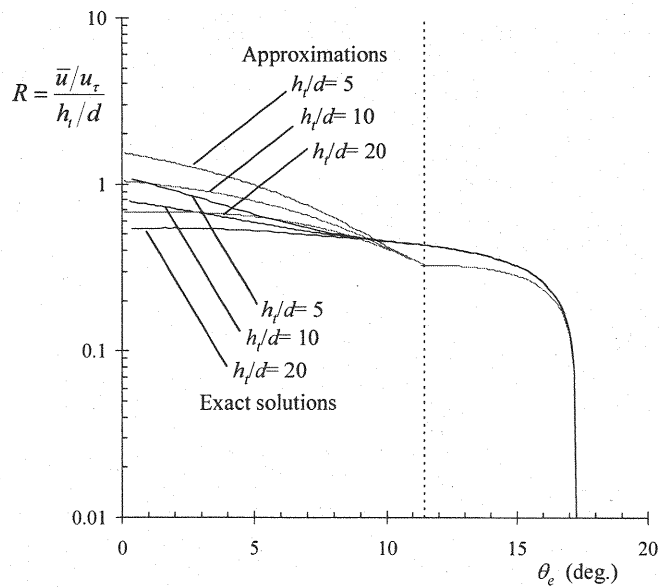


Fig. 5 Comparison of flow resistance, R , in between exact solutions and approximated solutions

$$\frac{\bar{u}}{u_\tau} = \frac{2}{5} \frac{h_t}{d} \left[\frac{(\sigma/\rho - 1)\bar{c} + 1 - (\bar{c}/c_*)^{1/3}(\sigma/\rho - 1)\bar{c} \tan \phi_s / \tan \theta}{f_d(\bar{c}) + f_f(\bar{c})} \right]^{1/2} \quad (16)$$

in which \bar{u} = cross sectional averaged velocity; u_τ = shear velocity on the bed surface defined as $u_\tau = \sqrt{gh_t \sin \theta}$; $f_d(\bar{c}) = k_d(1 - e^2)(\sigma/\rho)\bar{c}^{1/3}$; and $f_f(\bar{c}) = k_f(1 - \bar{c})^{5/3}\bar{c}^{-2/3}$.

In case of sediment flow, as mentioned above, the mean value of sediment concentration in the hyper-concentrated layer is approximately treated as $c_*/2$. Then, the approximated equations for flow characteristics such as velocity distribution, depth-averaged velocity and flux sediment concentration are analytically obtained by similar derivation shown in Eq. (16) (11).

Figure 5 shows the flow resistance and illustrates the differences obtained by exact solution and approximated solution, respectively. Herein, the parameter, R , is defined as $(\bar{u}/u_\tau)/(h_t/d)$ in the figure. As mentioned above, though there are some differences between the exact solution and the approximated solution, averaged quantities such as the flow resistance and sediment concentration reveal a little difference between those solutions.

Flow characteristics such as velocity and sediment concentration are evaluated as depth-averaged quantities in the numerical simulation using depth-averaged governing equations for a sediment-water mixture. Numerical treatments can be quite easy if the equation for a bed shear stress is analytically obtained in the momentum and mass conservation equations. In present study, the equations obtained based on exact solutions are used for equations of flow resistance for sediment flow and sediment flux concentration in computations taking into account the convenience for calculation of flow resistance in numerical simulations (11).

Correction Factor of Sediment Concentration and Velocity Profiles

The ratio of c_f/\bar{c} in one-dimensional flow equation is defined as a correction factor, γ , which is usually discussed in a suspended flow. It is calculated by using the profiles of sediment concentration and velocity derived by Eqs (13) and (14) in the steady and longitudinally uniform flow over an erodible bed (11). Referring to Fig. 6, the velocity and sediment concentration are expressed as follows:

$$u(z) = \bar{u} + u'(z), \quad c(z) = \bar{c} + c'(z) \quad (17)$$

in which \bar{u} and \bar{c} = cross sectional mean velocity and sediment concentration, and while u' and c' are the deviations from the mean velocity and sediment concentration, note that the deviations, u' and c' so defined satisfy $\int_0^{h_t} u' dz = 0$ and $\int_0^{h_t} c' dz = 0$. Substituting Eqs. (17) into the definition of sediment discharge rate, q_s , yields the following equation:

$$q_s = \int_0^{h_t} c u dz = \int_0^{h_t} (\bar{c} + c')(\bar{u} + u') dz = \int_0^{h_t} (\bar{c}\bar{u} + c'u') dz = \bar{c}\bar{u} \int_0^{h_t} \left(1 + \frac{c'u'}{\bar{c}\bar{u}}\right) dz \quad (18)$$

Defining the definition of c_f , we also have an equation.

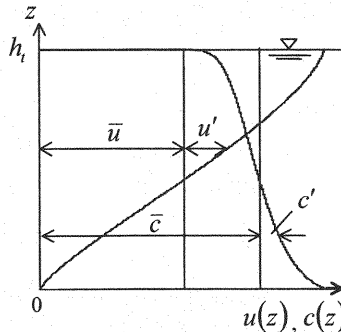


Fig. 6 Definition of mean value and deviation of velocity and sediment concentration

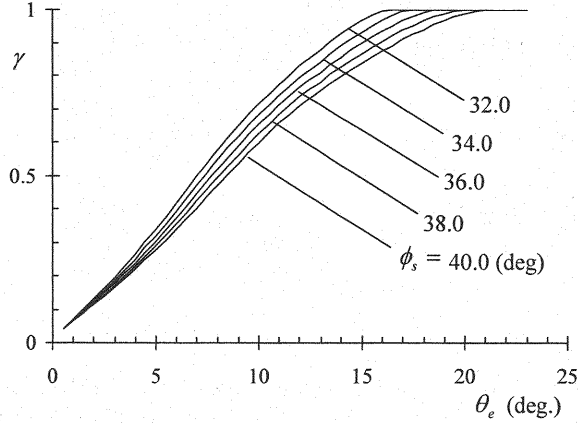


Fig. 7 Computed results of the relation between correction factor, γ , and bed slope

$$q_s = c_f q_m = c_f \bar{u} h \quad (19)$$

We conclude by comparing the relationships of Eqs. (18) and (19) that γ may be expressed.

$$\gamma \equiv \frac{1}{h} \int_0^h \left(1 + \frac{c' u'}{\bar{c} \bar{u}} \right) dz \left(= \frac{c_f}{\bar{c}} \right) \quad (20)$$

Figure 7 shows the values of γ computed by the exact solution and the approximation, respectively. In the figure, curves are drawn for various values of the interparticle friction angle, ϕ_s . The values of γ monotonically increase with the bed slope and depend significantly on ϕ_s .

SIMULATIONS OF DEBRIS FLOW AND THEIR APPLICATIONS

Governing Equations

We can discuss numerical simulations based on depth-averaged governing equations for a sediment-water mixture, considered as a single phase, as developed by Honda and Egashira (4, 5). Referring to Fig. 1, the continuity equation of sediment-water mixture, the continuity equation of sediment volume and the momentum conservation equation of sediment-water mixture are respectively written as follows:

$$\frac{\partial h_t}{\partial t} + \frac{\partial M}{\partial x} = \frac{E}{c_s} \quad (21)$$

$$\frac{\partial \bar{c} h_t}{\partial t} + \frac{\partial \gamma \bar{c} M}{\partial x} = E \quad (22)$$

$$\frac{\partial M}{\partial t} + \frac{\partial \beta \bar{u} M}{\partial x} = -gh \frac{\partial H}{\partial x} - \frac{\tau_b}{\bar{\rho}_m} \quad (23)$$

in which E = erosion rate of bed sediment; h_t = flow depth; H = height from a reference plane to the water surface ($H \cong h_t + z_b$); z_b = bed elevation; M = flux of sediment-water mixture in the flow direction defined as $M = \bar{u} h_t$; \bar{u} = cross sectional averaged velocity; γ = correction factor according for the distributions of sediment concentration and velocity; β = correction factor of momentum; and $\bar{\rho}_m$ = cross sectional averaged mass density of sediment and water mixture. The erosion rate, E , is related to the temporal change rate of bed elevation, $\partial z_b / \partial t$.

$$\frac{\partial z_b}{\partial t} = -\frac{E}{c_* \cos \theta}; \quad \sin \theta = -\frac{\partial z_b}{\partial x} \quad (24)$$

The constitutive equations for E and τ_b are expressed as follows (4):

$$\frac{E}{\bar{u}} = c_* \tan(\theta - \theta_e); \quad \tan \theta_e = \frac{(\sigma/\rho - 1)\bar{c} \tan \phi_s}{(\sigma/\rho - 1)\bar{c} + 1} \quad (25)$$

$$\tau_b = \tau_{y0} + \rho f_b |\bar{u}| \bar{u} \quad (26)$$

in which τ_{y0} = yield shear stress on the bed surface; and f_b = friction factor. We apply the friction factor obtained using the exact solution for velocity and sediment concentration profiles in the sediment flow regime in order to simplify the numerical calculation (11) as mentioned in former chapter, while, the following friction factor obtained analytically is applied for the debris flow regime:

$$f_b = \frac{25}{4} \{f_d(\bar{c}) + f_f(\bar{c})\} \left(\frac{h_t}{d}\right)^{-2} \quad (27)$$

The definitions for $f_d(\bar{c})$ and $f_f(\bar{c})$ are shown in Eq. (16).

Sediment Runoff Volume Transported by Debris Flow

Flume data obtained by the authors are used in order to discuss the importance of γ on the sediment discharge volume in numerical simulations. Flume tests are conducted in a rectangular open channel, which is shown in Fig. 8, 12 m long, 0.1 m wide and 0.2 m in deep, having a bed slope of 10 degrees. The parameters describing the sand are $c_* = 0.512$, $d = 0.218$ cm, $\phi_s = 38.7$ deg. and $\sigma/\rho = 2.62$. The specific discharge of mixture supplied from the upstream end is $q_m = 100$ cm²/s, while the sediment flux concentration is 0.01. Steady and longitudinally uniform debris flows is formed in the upper reach so as to erode a 10.0 cm high sediment bed in the downstream reach. The bed slope is steeper than the equilibrium bed slope of debris flow coming from upstream. The values of q_m , q_s and c_f are measured at intervals of 2.0 seconds at the downstream end.

Numerical simulations are conducted using Eqs. (21) to (26) and equation for flow resistance. The values of correction factor, γ , in Eq. (22) are specified based on the results of numerical computations as shown in Fig. 7. In the computation, the parameters of sand particles are the same ones used in experiments, and the leap-frog scheme is employed with $\Delta x = 0.02$ m and $\Delta t = 0.00005$ seconds.

Figure 9 shows a comparison between the calculated and experimental results concerning to the sediment discharge rate at the downstream end. Curves for c_f and \bar{c} , which are obtained introducing the values shown in Fig. 7 into γ in Eq. (22), are shown. The computed curve without γ is also shown in the figure ($\gamma = 1.0$). In order to compare calculated and experimental data, the time when the debris flow reaches the downstream end is set to zero. In the case that the correction factor, γ , is used for the computation, the calculated result for $c_f(t)$ at the

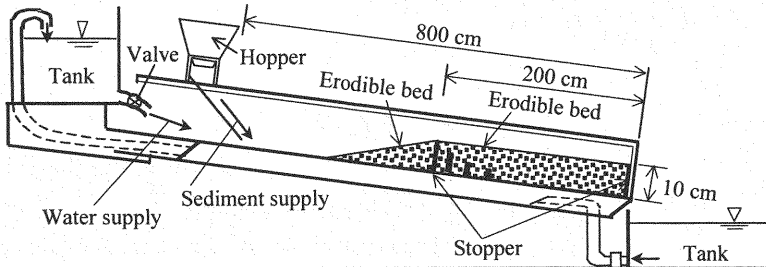


Fig. 8 Open channel used for experiment focused on erosion by debris flow

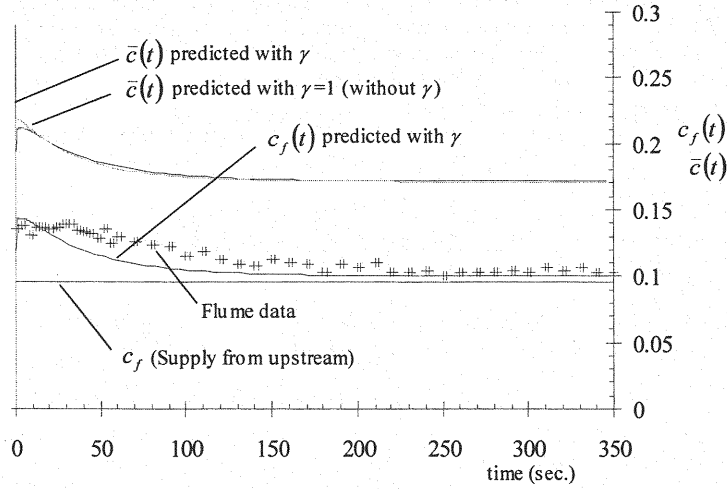


Fig. 9 Comparison between calculated and experimental data

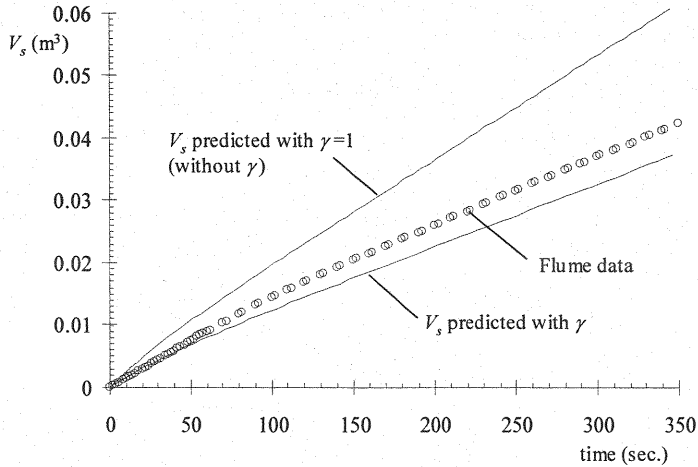


Fig. 10 Comparison of the calculated results for sediment runoff volume at the downstream end with and without a correction factor

downstream end agrees with flume data. Figure 10 shows a comparison of accumulated sediment volume at the down stream end for the case $\gamma = 1.0$ (without a correction factor) and $\gamma \neq 1.0$ (with a correction factor). Flume data shown in Fig. 9 are plotted in the figure. Calculated sediment volume without γ is much greater than sediment volume obtained with γ . On the other hand, sediment volume computed numerically with γ agree with flume data, though there is rather discrepancy between computation and flume data. Those results suggest that the effect of γ on the sediment runoff volume at an arbitrary section plays a significant role in predicting some debris flow events. In previous author's research, it was suggested that the effect of the potential depth of sediment erosion on the outflow of sediment transported by debris flow is significant, and that its depth needs to be evaluated precisely. Additionally, in estimating sediment runoff volume transported by debris flows, the importance of the correction factor associated with velocity and sediment concentration profiles should be noted.

CONCLUSIONS

Flume tests and experiments were conducted to investigate the importance of correction factor associated with the profiles of velocity and sediment concentration. The results are summarized as follows:

- (1) A correction factor, γ , expressing the ratio of the flux sediment concentration to the cross sectional averaged sediment concentration, \bar{c} , is derived using our constitutive equations of debris flow in steady and uniform flow.
- (2) Numerical simulations for the bed erosion by debris flow over erodible bed were conducted by using the

correction factor. These results were compared with flume data in order to investigate the validity of the correction factor. The predicted flux sediment concentration agrees with flume data. The importance of introducing the correction factor into the continuity equation of sediment is shown by numerical simulation and flume data.

(3) Sediment transportation is overestimated when the effect of sediment concentration profile is not taken into account. These results emphasize that the correction factor plays an important role in debris flow simulation. Additionally, it can play a significant role in the flow regime of the sediment flow and the flow with bed loads.

ACKNOWLEDGMENTS

Parts of this study are supported by Grant-in-Aid for Scientific Research of Young Scientists (B) from the Japanese Ministry of Education, Culture, Sports, Science and Technology. Helpful discussions with K. Miyamoto, University of Tsukuba, are gratefully acknowledged. In addition, the authors should be grateful to Mr. Shogo Kuroda, Mr. Yusuke Etoh and Mr. Keisuke Yoshida, who were graduate students of Ritsumeikan University and made valuable support for experiment and their analyses in this study.

REFERENCES

1. Itoh, T., and S. Egashira: Comparative study of constitutive equations for debris flows, *Journal of Hydrosience and Hydraulic Engineering*, Vol.17, No.1, pp.59-71, 1999.
2. Egashira, S., K. Miyamoto and T. Itoh: Bed-load rate in view of two phase flow dynamics, *Ann. Jour. Hydr. Eng., JSCE*, 41, pp.789-797, 1997, (in Japanese).
3. Egashira, S., K. Miyamoto and T. Itoh: Constitutive equations of debris flow and their applicability, *Proceedings of 1st International Conference of Debris-Flow Hazards Mitigation; Mechanics, Prediction and Assessment* (Chen, C.C. ed.), New York, ASCE, pp.340-349, 1997.
4. Egashira, S., N. Honda and T. Itoh: Experimental study on the entrainment of bed material into debris flow, *Phys. Chem. Earth (C)*, Vol.26, No.9, pp.645-650, Elsevier, 2001.
5. Honda, N. and S. Egashira: Prediction of debris flow characteristics in mountainous torrents, *Proceedings of 1st International Conference of Debris-Flow Hazards Mitigation; Mechanics, Prediction and Assessment* (Chen, C.C. ed.), New York, ASCE, pp.707-716, 1997.
6. Hashimoto, H., K. Park and M. Hirano: Numerical simulation of small-discharge debris-flows at Mt. Unzendake, *Debris-Flow Hazards Mitigation: Mechanics, Prediction and Assessment* (Wieczorek, G.F. & Naeser, N.D. ed.), Rotterdam, Balkema, pp.177-183, 2000.
7. Nakagawa, H., T. Takahashi and Y. Satofuka: A debris flow disaster on the fan of the Harihara River, Japan, *Debris-Flow Hazards Mitigation: Mechanics, Prediction and Assessment* (Wieczorek, G.F. & Naeser, N.D. ed.), Rotterdam: Balkema, pp.93-201, 2000.
8. Takahama, J., Y. Fujita and Y. Kondo: Analysis method of transitional flow from debris flow to sediment sheet flow, *Annual Jour. of Hydraulics Engineering, JSCE*, pp.683-686, 2000 (in Japanese).
9. Egashira, S., T. Itoh, K. Miyamoto and N. Honda: Importance correction factor associated with sediment concentration profile in debris flow simulation, *Proceedings of the Second International Symposium on Flood Defence*, Vol.II, pp.1658-1666, 2002.
10. Miyamoto, K.: *Mechanics of grain flows in Newtonian fluid*, Ph.D.-thesis, Ritsumeikan Univ., 1985 (in Japanese).
11. Itoh, T.: *The study on the constitutive equations of debris flow and their applicability*, Ph.D. thesis, Ritsumeikan Univ., 2001 (in Japanese).

APPENDIX-NOTATION

The following symbols are used in this paper:

- | | |
|-----------|--|
| c | = sediment concentration by volume in mixture; |
| \bar{c} | = cross sectional averaged sediment concentration; |
| c' | = deviations from the mean sediment concentration; |
| c_n | = sediment concentration by volume in the non-flowing layer; |
| c_s | = representative value of sediment concentration in sediment moving layer; |
| d | = sediment particles size; |

e	= restitution coefficient of particle to particle;
f_d	= coefficient of shear stress due to inelastic collisions of particle to particle;
f_f	= coefficient of shear stress due to shearing interstitial water;
f_b	= friction factor
g	= acceleration due to gravity;
h_t	= flow depth;
h_s	= thickness of sediment moving layer;
H	= height from a reference plane to the water surface ($H = h + z_b$);
k_d	= constant by Egashira et al. ($k_d = 0.0828$);
k_f	= empirical constant by Egashira et al. ($k_f = 0.16 - 0.25$);
M	= flux of sediment-water mixture in the flow direction;
p	= isotropic pressure;
p_d	= dynamic pressure due to inelastic particle collisions;
p_s	= pressure of static interparticle contacts;
p_w	= pressure of water;
q_s	= sediment discharge rate;
u	= local mean velocity;
\bar{u}	= cross sectional averaged velocity;
u_τ	= shear velocity on the bed surface, $u_\tau = \sqrt{gh_t \sin \theta}$;
u'	= deviations from the mean velocity;
z	= bed normal coordinate;
z_b	= bed elevation;
β	= correction factor of momentum;
γ	= correction factor according for the distributions of sediment concentration and velocity;
θ	= inclination from horizontal line;
ρ	= mass density of water;
ρ_m	= mass density of sediment mixture, $\rho_m = (\sigma - \rho)c + \rho$;
$\bar{\rho}_m$	= cross sectional averaged mass density of sediment and water mixture;
σ	= mass density of sediment particles;
τ	= sheer stress at any distance from the bed surface;
τ_b	= shear stress on the bed surface;
τ_d	= shear stress due to inelastic particle to particle collisions;
τ_f	= shear stress supported by interstitial water;

- τ_y = yield stress;
- τ_{y0} = yield shear stress on the bed;
- τ_w = shear stress on the boundary between the sediment moving layer and the clear water layer;
- τ_* = dimensionless shear stress; and
- ϕ_s = interparticle friction angle of sediment particles.

(Received July 1, 2004 ; revised August 22, 2005)